NUCL SCI TECH (2017) 28:114
DOI 10.1007/s41365-017-0260-5

Two-plane painting injection scheme for BRing of HIAF

Guo-Feng Qu[1,2] · Wei-Ping Chai[1] · Jia-Wen Xia[1] · Jian-Cheng Yang[1] · Heng Du[1,2] · Zhong-Shan Li[1,2] · Wen-Wen Ge[1,2] · Wen-Heng Zheng[1,2] · Peng Shang[1,2]

Received: 12 December 2016 / Revised: 9 January 2017 / Accepted: 19 January 2017 / Published online: 5 July 2017

Abstract The high-intensity heavy-ion accelerator facility (HIAF) is under design at the Institute of Modern Physics (IMP) and will provide an intense ion beam for nuclear physics, atomic mass measurement research, and other applications. As the main ring of HIAF, the BRing accumulates beams to high intensity and accelerates them to high energy. To achieve high intensities up to 1×10^{11} ($^{238}U^{34+}$), the injection gain of the BRing must be as high as 88. However, multiple multiturn injection supported by the electron cooling system takes a long time, causing substantial beam loss under a strong space charge effect. Hence, a two-plane painting injection scheme is proposed for beam accumulation in the BRing. This scheme uses a tilted injection septum and horizontal and vertical bump magnets to paint the beam into horizontal and vertical phase space simultaneously. In this paper, the two-plane painting injection parameters are optimized, and the resulting injection process is simulated using the Objective Ring Beam Injection and Tracking (ORBIT) code. An injection gain of up to 110.3 with a loss rate of 2.3% is achieved, meeting the requirements of BRing.

Keywords HIAF · Heavy-ion accelerator · Two-plane painting injection · Genetic algorithm · ORBIT

This work was supported by the National Natural Science Foundation of China (No. 11505256).

✉ Wei-Ping Chai
chaiwp@impcas.ac.cn

[1] Institute of Modern Physics, Chinese Academy of Sciences, Lanzhou 730000, China

[2] University of Chinese Academy of Sciences, Beijing 100046, China

1 Introduction

The high-intensity heavy-ion accelerator facility (HIAF) is under design at the Institute of Modern Physics [1]. HIAF consists of a superconducting electron cyclotron resonance ion source (SECR), an ion Linac accelerator (iLinac), a booster ring (BRing), and a spectrometer ring (SRing) [2–4]. It provides an intense ion beam for high-energy density physics, nuclear physics, atomic mass measurement research, and other applications.

As the main ring of HIAF, BRing accumulates the beams from iLinac to high intensity and accelerates them to high energy. The layout of BRing is shown in Fig. 1, and the basic parameters are listed in Table 1. The design intensity of BRing is 1×10^{11} ($^{238}U^{34+}$). By calculation, to accumulate beams up to the design intensity of BRing, the injection gain must reach 88, where the injection gain is defined as the ratio of the retained beam current in the ring to the incoming beam current. For a heavy-ion synchrotron accelerator, a typical injection scheme is multiple multiturn injection, which is a combination of one-plane painting injection and an electron cooling system. However, the space charge effect is strong in the high-intensity heavy-ion synchrotron. In the multiple multiturn injection scheme, the electron cooling system makes the particles shrink to a small size, further increasing the space charge effect. Moreover, during multiple multiturn injection, the electron cooling process takes a long time (typically several seconds [5]). The combination of the strong space charge effect and the long duration causes substantial beam loss, which creates many problems with respect to maintenance, vacuum, and heat. Hence, the multiple multiturn injection scheme is not suitable for BRing.

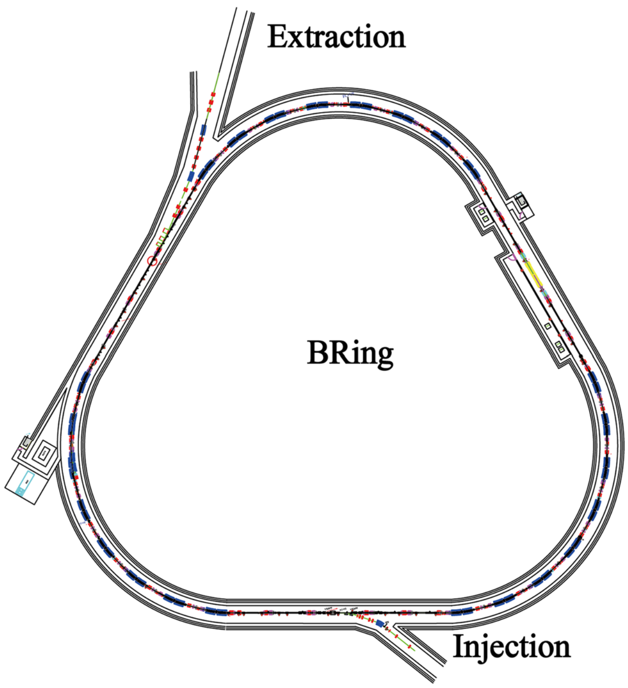

Fig. 1 (Color online) Layout of BRing

Table 1 Basic parameters of BRing

Circumference (m)	440.2
Acceptance of the ring (π mm mrad)	250,100
Number of accumulated particles	1×10^{11} ($^{238}U^{34+}$)
Injection current (pmA)	0.028 ($^{238}U^{34+}$)
Injection energy (MeV/u)	25 ($^{238}U^{34+}$)
Emittance of injected beam (π mm mrad)	5,5
Momentum spread at injection	±0.005
Extraction energy (MeV/u)	800 ($^{238}U^{34+}$)

To inject enough particles into BRing with a low beam loss, a two-plane painting injection scheme is proposed [6]. The two-plane painting injection scheme was first proposed by C.R. Prior for the heavy-ion-driven ignition facility (HIDIF) in 1998, but it has not been applied because HIDIF is not actually constructed [7]. In the two-plane painting injection scheme, the beam is painted simultaneously in the horizontal and vertical phase space in the ring. This scheme makes full use of the acceptance of the ring to accumulate many more particles than a typical one-plane painting injection. It does not need an electron cooling process and hence has a short injection duration of about 1 ms. In addition, it can obtain a more uniform beam distribution, which can weaken the space charge effect [8]. The short injection duration and the weak space charge effect reduce the risk of beam loss.

In this paper, the two-plane painting injection scheme is introduced in Sect. 2. The physical analysis is described in Sect. 3. Optimization and simulation are covered in Sects. 4 and 5, respectively. A summary is given in Sect. 6.

2 The two-plane painting injection scheme

In the two-plane painting injection system, two aspects are set differently from typical one-plane painting injection. First, four horizontal bump magnets and four vertical bump magnets are located in the injection section, as shown in Fig. 2. During the injection process, they generate a locally bumped orbit. Second, the injection septum is set tilted on its corner, as shown in Fig. 3 [9]. Because the injection septum is set tilted on its corner, the circulating beam will survive if it avoids the injection septum in either of the horizontal and vertical directions.

The injection process is shown in Fig. 4. At the beginning of the injection, a locally bumped orbit is generated near the injection septum, and the first slice of beam is injected into the ring, as shown in Fig. 4(1). The injected beam then undergoes betatron oscillations in both the horizontal and vertical planes. One revolution later, the first slice of beam will once again enter the injection section. Due to betatron oscillations, the first slice of beam will avoid hitting the injection septum this time, as shown in Fig. 4(2). Meanwhile, a new slice of beam will be injected into the ring, and the bumped orbit will descend at the same time. After a few revolutions, when the first slice of beam comes back to the injection septum, the bumped orbit has moved down, and hence, the first slice of beam avoids hitting the injection septum and survives in the ring, as shown in Fig. 4(3). The process is repeated until the injection is complete.

3 Physical analysis

During the injection process, the positions of the injected particles are determined by the following equation [10]:

$$X_n = X_{co,n} + A_x * \sin(\phi_{x0} + 2\pi * Q_x * n), \quad (1)$$

$$Y_n = Y_{co,n} + A_y * \sin(\phi_{y0} + 2\pi * Q_y * n), \quad (2)$$

where X_n and Y_n are the horizontal and vertical positions of the injected particles when they pass by the injection septum at the nth turn. $X_{co,n}$ and $Y_{co,n}$ represent the horizontal and vertical amplitudes of the bumped orbit at the nth turn. A_x and A_y are the horizontal and vertical betatron

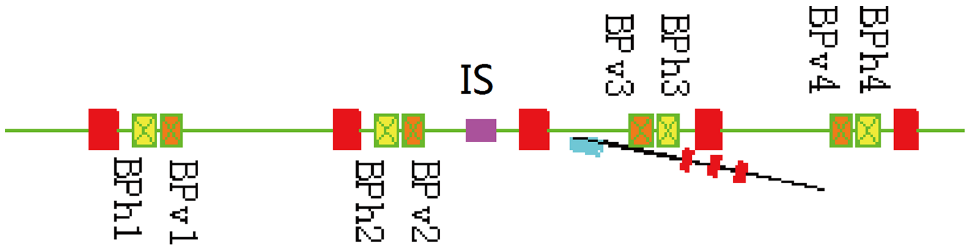

Fig. 2 (Color online) Injection section of BRing. IS is an injection septum; BPh is a horizontal bump magnet; BPv is a vertical bump magnet

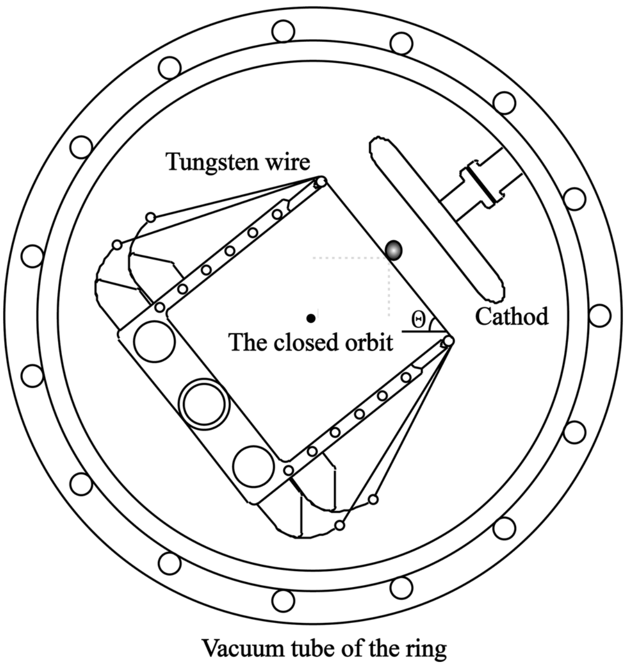

Fig. 3 Injection septum. Θ is the tilt angle of the injection septum

oscillation amplitudes. ϕ_{x0} and ϕ_{y0} are the horizontal and vertical initial phases, Q_x and Q_y are the horizontal and vertical tunes, and n is the number of turns. A_x, A_y, ϕ_{x0}, and ϕ_{y0} are determined by the position and direction of the incoming beam with respect to the bumped orbit as the beam is injected into the ring and by the Twiss parameters of the ring at the injection point.

The injection septum can be described as:

$$a * x + b * y = c, \tag{3}$$

where a and b meet the equation

$$a^2 + b^2 = 1. \tag{4}$$

It can be seen that if the inequality

$$a * X_n + b * Y_n \geq c, \tag{5}$$

holds, the particle will hit the injection septum or else enter the injection channel and be impacted by the electric field of the injection septum. These particles will be lost in the injection septum or downstream after the injection septum. Substituting Eqs. (1) and (2) into Eq. (5):

$$\begin{aligned} & a * (X_{\mathrm{co,n}} + A_x * \sin(\phi_{x0} + 2\pi * Q_x * n)) \\ & + b * (Y_{\mathrm{co,n}} + A_y * \sin(\phi_{y0} + 2\pi * Q_y * n)) \geq c, \end{aligned} \tag{6}$$

For convenience of discussion, $L_{\mathrm{co,n}}$ and $L_{\mathrm{osc,n}}$ are defined as:

$$L_{\mathrm{co,n}} = a * X_{\mathrm{co,n}} + b * Y_{\mathrm{co,n}}, \tag{7}$$

$$\begin{aligned} L_{\mathrm{osc,n}} &= a * (A_x * \sin(\phi_{x0} + 2\pi * Q_x * n)) \\ &\quad + b * (A_y * \sin(\phi_{y0} + 2\pi * Q_y * n)), \end{aligned} \tag{8}$$

and

$$L_{\mathrm{osc,n,max}} = \max_{1<i<m} \left\{ {}^{i}L_{\mathrm{osc,n}} \right\}, \tag{9}$$

where m is the number of circulating particles and ${}^{i}L_{\mathrm{osc,n}}$ is the $L_{\mathrm{osc,n}}$ of the i_{th} particle. The physical meaning of $L_{\mathrm{co,n}}$ and $L_{\mathrm{osc,n,max}}$ is shown in Fig. 5.

When $L_{\mathrm{co,n}}$ and $L_{\mathrm{osc,n,max}}$ satisfy the inequality:

$$L_{\mathrm{co,n}} + L_{\mathrm{osc,n,max}} \geq c, \tag{10}$$

beam loss occurs. To avoid beam loss, the amplitude of the bumped orbit must satisfy:

$$L_{\mathrm{co,n+1}} = \begin{cases} L_{\mathrm{co,n}} & L_{\mathrm{co,n}} + L_{\mathrm{osc,n+1,max}} \leq c \\ c - L_{\mathrm{osc,n+1,max}} & L_{\mathrm{co,n}} + L_{\mathrm{osc,n+1,max}} > c \end{cases}, \tag{11}$$

As the value of Lco decreases, the linear displacement between the incoming beam and the bumped orbit increases. When the increased displacement makes it impossible to capture the incoming beam fully into the acceptance of the ring, the two-plane painting injection process ends. Obviously, to achieve high injection gain, the injection parameters and the bump curves should be optimized to slow down the decrease in amplitude of the bumped orbit.

4 Optimization

The injection parameters and bump curves were optimized using a linear particle-tracking code developed in MATLAB. In this code, the space charge effect was considered as a fixed tune shift per turn for each particle. The value of the tune shift was calculated using the ORBIT code [11, 12].

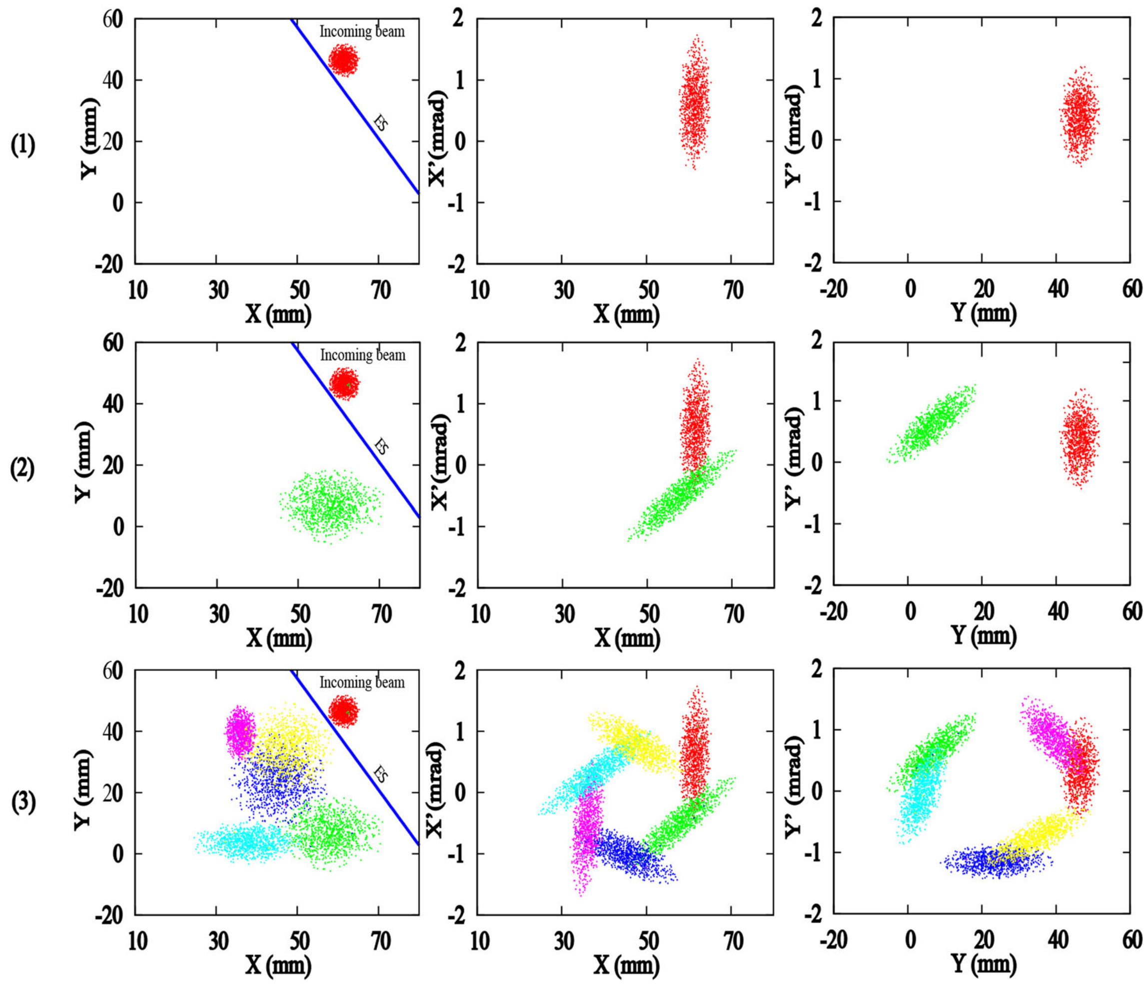

Fig. 4 (Color online) Injection process

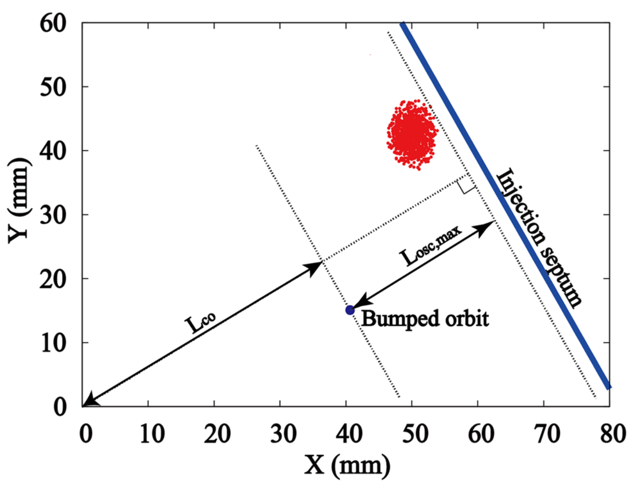

Fig. 5 (Color online) Physical meaning of $L_{\mathrm{co,n}}$ and $L_{\mathrm{osc,n,max}}$. The origin coordinates (0, 0) represent the ideal orbit

In the two-plane painting injection scheme, the angle of incoming beam relative to the bumped orbit affects the injection. Therefore, the direction of the incoming beam needs to be optimized, while the direction of the bumped orbit is kept parallel to the ideal orbit. For the same reason, the position of the bumped orbit needs to be optimized, while the position of the incoming beam is kept immediately beside the injection septum. In summary, the injection parameters to be optimized include the direction of the incoming beam, x' and y', the Twiss parameters of the incoming beam, β_{xi}, β_{yi}, α_{xi}, and α_{yi}, the Twiss parameters of the ring at the injection point, $\beta_{xm}, \beta_{ym}, \alpha_{xm}, \alpha_{ym}$, the machine working point, Wp_x and Wp_y, the tilt angle of the injection septum, Θ, and the bump curves.

The injection gain can be considered as a function of all the injection parameters mentioned above. In this research, it is found that how the value of the function changes with respect to each injection parameter is affected by other injection parameters. So it is impossible to achieve the highest injection gain by tuning each of the injection parameters separately. To achieve the highest injection gain, it is necessary to tune all the injection parameters simultaneously to find the optimal injection parameter

Table 2 Optimal injection parameters

Machine working point (horizontal/vertical)	8.1704/7.6374
Twiss parameters of the ring at the injection section	$\alpha_{xm} = -0.24$; $\alpha_{ym} = -0.16$; $\beta_{xm} = 13.212\,\text{m}$; $\beta_{ym} = 18.846\,\text{m}$
Twiss parameters of the incoming beam	$\alpha_{xi} = 0.065$; $\alpha_{yi} = -0.060$; $\beta_{xi} = 3.586\,\text{m}$; $\beta_{yi} = 6.943\,\text{m}$
Direction of the incoming beam [horizontal (mrad)/vertical (mrad)]	0.6/0.3
Tilt angle of the injection septum (°)	66
Duration of injection	113 revolution periods (0.73 ms)

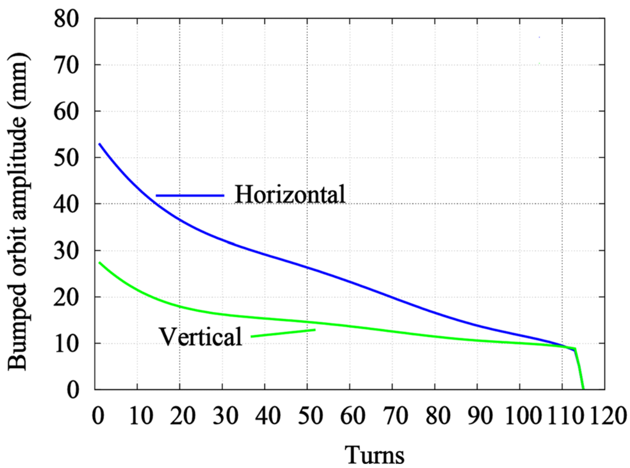

Fig. 6 (Color online) Optimal route of the bumped orbit and bump curves

combination. For an optimization problem with dozens of variables, the computing load to perform an overall comparison of all possible combinations is obviously unacceptable. Instead, a genetic algorithm was used in this optimization [13–15]. The genetic algorithm is an optimization algorithm that is effective in optimizing multi-variable objective functions and offers fast search capability.

The optimized injection parameters are listed in Table 2, and the optimized bump curve is shown in Fig. 6. As the optimized injection parameters are given, a new lattice is generated to match the Twiss parameters and working point by tuning a few quadrupoles in WINAGILE program. All the results described below are based on this information.

5 Simulation

The injection process based on the optimized parameters given above was simulated using the ORBIT code. In total, 1000 macroparticles per turn are injected into the ring to model the injected beam. Transverse Gaussian distribution is taken. As the RF system of BRing does not work during injection, the longitudinal uniform distribution is taken for

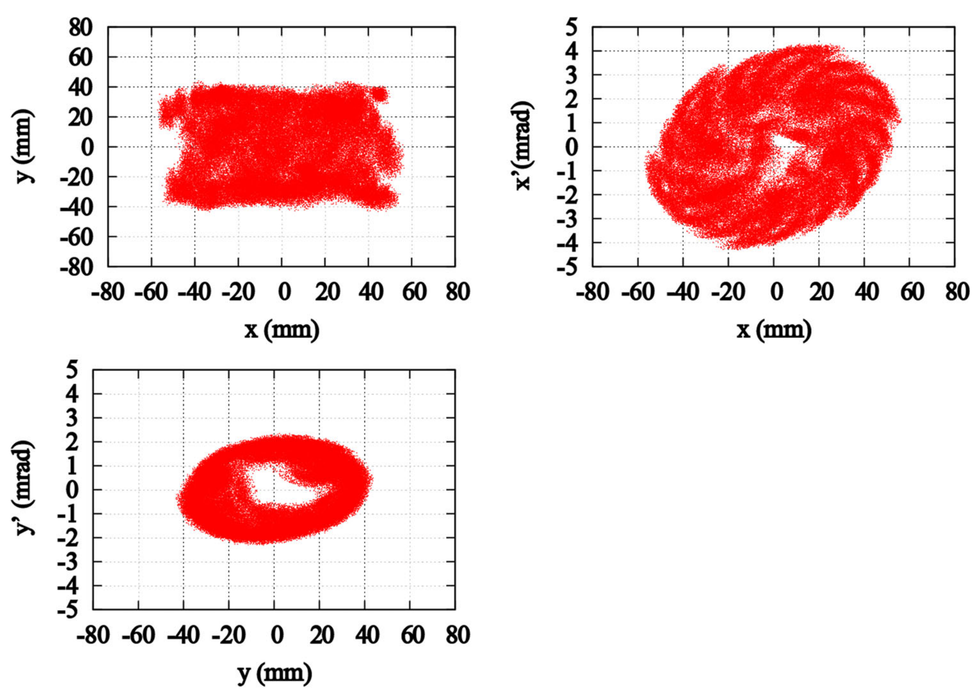

Fig. 7 (Color online) Transverse distribution of retained particles. The *top left figure* is the beam distribution in transverse real space. The *top right figure* is the beam distribution in the horizontal phase space. The *bottom left figure* is the beam distribution in the vertical phase space. In the three figures, X is the horizontal position, Y is the vertical position, X' is the horizontal angle, and Y' is the vertical angle

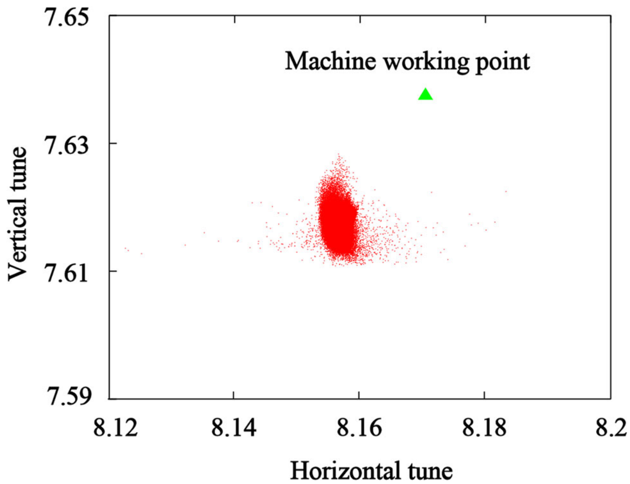

Fig. 8 (Color online) Tune of the retained particles. The *red dots* represent the particles. The horizontal coordinate of a *dot* is the horizontal tune of the particle, and the vertical coordinate of the *dot* is the vertical tune of the particle

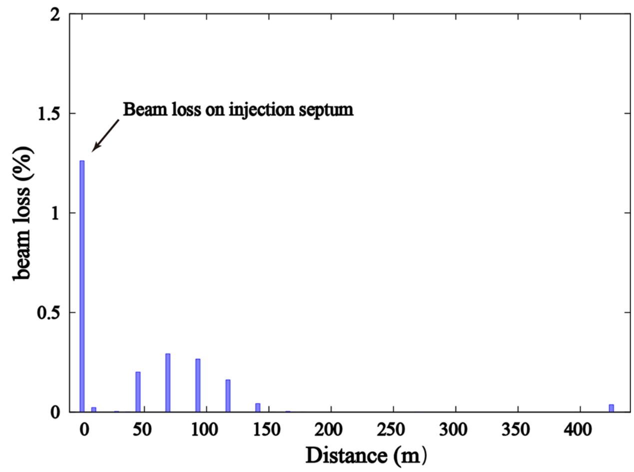

Fig. 10 (Color online) Beam loss distribution along the ring. 'Distance' is the distance from the injection point in the downstream direction. The zero point of 'Distance' represents the injection point into the ring

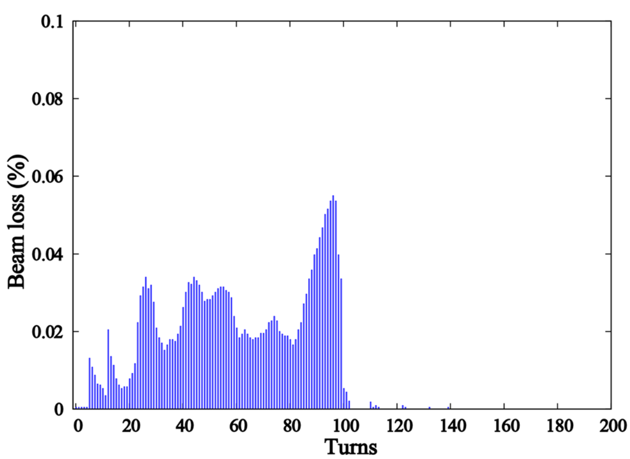

Fig. 9 (Color online) Beam loss during injection

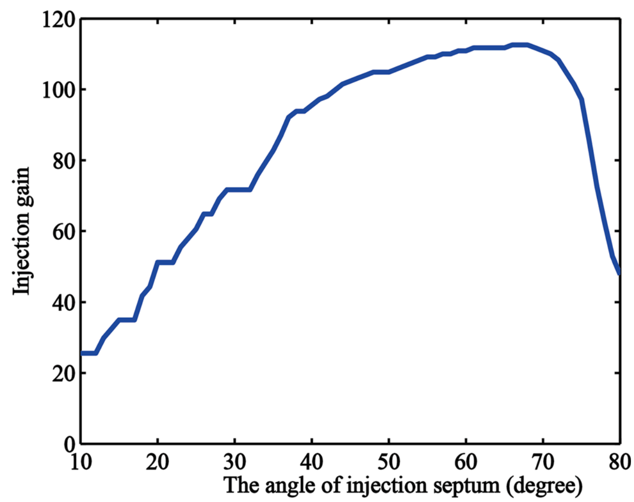

Fig. 11 (Color online) Relationship between injection gain and injection septum tilt angle

the injected beam in this simulation. The momentum deviation is 5‰ and a Gaussian momentum distribution is used. The space charge effect was included and calculated using the PIC method [16, 17]. An injection gain of up to 110.3 with a beam loss rate of 2.3% was achieved. The transverse distribution of the retained beam is shown in Fig. 7. It is apparent that the retained beam is relatively uniformly distributed in the acceptance of the ring. The relatively uniform particle distribution weakens the space charge effect and then reduces the tune shift of retained particles.

Figure 8 shows that the horizontal and vertical tunes of the retained particles are shifted by about −0.015, −0.020 from the machine operating point and are spread over an area with horizontal size 0.008 and vertical size 0.016. The low tune shift reduces the probability of crossing the resonance line and then lowering the beam loss.

After injection, the retained particles continued to be tracked for 70 turns. The beam loss as a function of the number of turns is shown in Fig. 9. Clearly, some beam loss happened after injection, although all particles were initially injected into the acceptance of the ring. This phenomenon was due to the space charge effect. The beam loss distribution along the ring is shown in Fig. 10.

Simulations were performed with various values of the main injection parameters. Figure 11 shows the relationship between injection gain and the tilt angle of the injection septum. A smaller injection septum tilt angle was found to decrease beam loss due to the large horizontal profile presented. However, it also increased beam loss due to the large vertical profile. This experiment showed that

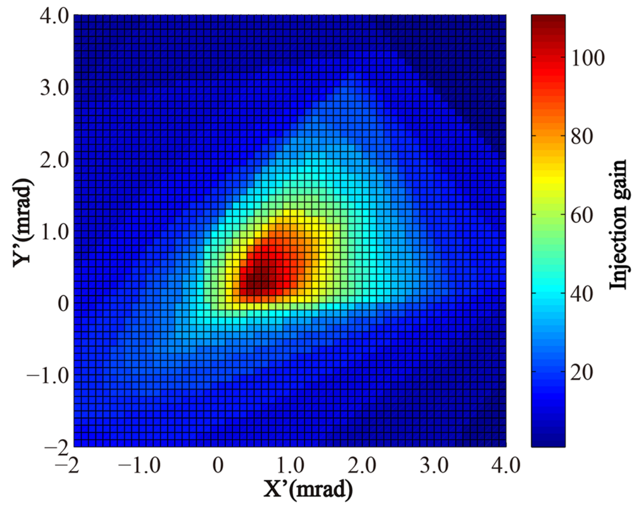

Fig. 12 (Color online) Relationship between injection gain and incoming beam direction

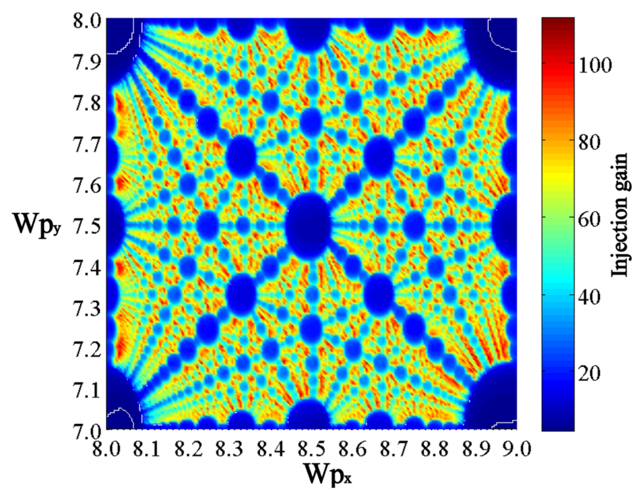

Fig. 13 (Color online) Relationship between injection gain and machine working point

the two-plane painting injection scheme has a large tolerance for variations in the tilt angle of the injection septum. A tilt angle between 36° and 75° can meet the requirement of BRing, with 66° being the best choice.

Figure 12 shows the relationship between injection gain and the direction of the incoming beam. The angle between the direction of the incoming beam and the direction of the bumped orbit determines the initial phase, ϕ_0, of the injected beam and therefore affects the injection gain. Figure 12 shows that the tolerance of the incoming beam direction is about 0.5 mrad.

Figure 13 shows the relationship between injection gain and machine working point. Clearly, there are many possible choices of working point to achieve a high injection gain. This provides convenience for the lattice design of BRing.

6 Summary

In this paper, the two-plane painting injection scheme has been studied. The injection parameters of the two-plane painting injection have been optimized. The resulting injection process has been simulated using the ORBIT code. An injection gain of up to 110.3 with a loss rate of 2.3% has been achieved. The results show that a two-plane painting injection scheme can meet the requirement of beam accumulation in the BRing of the HIAF.

References

1. J.C. Yang, J.W. Xia, G.Q. Xiao et al., High Intensity heavy ion Accelerator Facility(HIAF) in China. Nucl. Instrum. Methods B **317**, 263–265 (2013). doi:10.1016/j.nimb.2013.08.046
2. C. Li, L. Sun, Y. He et al., Conceptual design of LEBT and RFQ for the HIAF linac. Nucl. Instrum. Methods A **729**, 426–433 (2013). doi:10.1016/j.nima.2013.06.019
3. Y. Yang, L.T. Sun, X.Z. Zhang et al., Preliminary design of a LEBT for HIAF linac at IMP, TUPRO054, in *Proceedings of IPAC2014*, Dresden, Germany, pp. 1153–1155 (2014)
4. X. Gao, J.C. Yang, J.W. Xia et al., SHER-HIAF ring lattice design. Chin. Phys. C **38**(4), 84–87 (2014). doi:10.1088/1674-1137/38/4/047002
5. L.J. Mao, J.C. Yang, J.W. Xia et al., Electron cooling system in the booster synchrotron of the HIAF project. Nucl. Instrum. Methods A **786**, 91–96 (2015). doi:10.1016/j.nima.2015.03.052
6. C.R. Prior, *HIDIF Horizontal–Vertical Multi-Turn Injection, HIDIF/RAL2 CLRC* (Rutherford Appleton Laboratory, Chilton) (1997)
7. I. Hofmann, HIDIF-an approach to high repetition rate inertial fusion with heavy ions. Nucl. Instrum. Methods A **415**(1–2), 11–19 (1998). doi:10.1016/S0168-9002(98)00512-9
8. L.J. Laslett, On intensity limitations imposed by transverse space-charge effects in circular particle accumulators, in *Proceedings of 1963 Summer Study on Storage Rings, BNL-Report 7534*, pp. 324–367 (1963)
9. D.H. Kim, B.T. Jang, Design and construction of the CERN LEIR injection septa, in *21st Particle Accelerator Conference (PAC 05)*, pp. 2690–2692 (2005)
10. S.Y. Lee, *Accelerator Physics* (World Scientific, Singapor) (2004), pp. 47–50
11. J. Galambos, J. Holmes, D. Olsen, *ORBIT User Manual*, SNS technical note (1999)
12. J. Galambos, S. Danilov, D. Jeon et al., *ORBIT: A ring injection code with space charge* (1999)
13. A.C. David, *An Introduction to Genetic Algorithms For Scientists and Engineers* (World Scientific, Singapore) (1999)
14. C.R. Houck, J.A. Joines, M.G. Kay, *A Genetic Algorithm for Function Optimization: A MATLAB implementation*. Ncsu, 22 (1998)
15. A. Chipperfield, P. Fleming, H. Pohlheim et al., *Genetic algorithm toolbox for use with MATLAB* (1994). http://www.pohlheim.com/Papers/tr_gatbx12/ChipperfieldFlemingPohlheimFonseca_tr_GATbx_v12.pdf
16. R.W. Hockney, J.W. Eastwood, *Computer Simulation Using Particles* (Adam Hilger, IOP Publishing, New York) (1988)
17. J.D. Galambos, A.U. Luccio, D.K. Olsen et al., A particle-in-cell model for space charge dynamics in rings, in *6th European Particle Accelerator Conference*, Stockholm, Sweden, pp. 22–26 (1998)